

The Church of the Nativity in Bethlehem: Analysis of a Local Structural Consolidation

Claudio Alessandri & Jessica Turrioni

**International Journal of Civil
Engineering**

ISSN 1735-0522

Int J Civ Eng
DOI 10.1007/s40999-017-0148-0



 Springer

Your article is protected by copyright and all rights are held exclusively by Iran University of Science and Technology. This e-offprint is for personal use only and shall not be self-archived in electronic repositories. If you wish to self-archive your article, please use the accepted manuscript version for posting on your own website. You may further deposit the accepted manuscript version in any repository, provided it is only made publicly available 12 months after official publication or later and provided acknowledgement is given to the original source of publication and a link is inserted to the published article on Springer's website. The link must be accompanied by the following text: "The final publication is available at link.springer.com".

The Church of the Nativity in Bethlehem: Analysis of a Local Structural Consolidation

Claudio Alessandri¹  · Jessica Turrioni²

Received: 10 August 2016 / Revised: 2 January 2017 / Accepted: 9 January 2017
© Iran University of Science and Technology 2017

Abstract An innovative technique for reinforcing a wall of the Church of the Nativity in Bethlehem against earthquakes is proposed. The use of such a technique was required due to the peculiarity of the site, recently added to the UNESCO list of World Heritage sites, which is important to both Christian and Islamic religions. Local seismicity data and the parameters of an equivalent Italian site provided the input data for a design earthquake, and 3D modal analysis of the entire Church revealed that the structure is characterized by clear local modes of vibration. As per the most recent studies on masonry structures, local assessment based on limit analysis procedures was performed. This showed that in the event of an earthquake, a Crusader-era wall addition is at risk of collapse via simple overturning around its own base, due to the lack of firm connections with the orthogonal walls of the façade and the transept. Hence, a novel double system of horizontal steel tension structures was designed to consolidate the wall, conforming to the main restoration Charter requirements, i.e. lightness, non-invasiveness and reversibility, and being hidden from the sight of visitors. In the absence of reliable local regulations, all analyses, computations and checks on the proposed intervention were carried out with reference to the Italian technical regulations.

Keywords Tension structures · Masonry · Church of the Nativity · Local collapse mechanisms

✉ Claudio Alessandri
claudio.alessandri@unife.it

¹ Structural Mechanics, University of Ferrara, Via Saragat 1, 44122 Ferrara, Italy

² Department of Engineering, University of Ferrara, Via Saragat 1, 44122 Ferrara, Italy

1 Introduction

It is difficult to design interventions to safeguard historic buildings against structural damage, because it is necessary to collect data not only on their current state of conservation, but also on their past history, and the techniques used in their construction. Furthermore, all potential damage scenarios must be considered, but analysis of the structural response of the whole building to external loads is complicated by the non-linear behaviour of the materials involved, as well as uncertainties regarding their construction techniques, mechanical properties, and connections between structural elements (or lack thereof). Moreover, it is particularly vital to accurately assess the structural vulnerability of a historic building located in a seismic area. Factors that need to be taken into account are not only loading under the usual conditions (own weight, snow, wind, human traffic, etc.), but also the extremely complex conditions that occur during exceptional events like earthquakes.

This paper analyses the seismic vulnerability of just such a structure—a masonry wall of the Church of the Nativity in Bethlehem—and proposes a means of reinforcing it against local earthquakes in conformity to the principles and recommendations expressed by the main restoration Charters. This work is part of a wide-ranging project financially supported by the Palestinian National Authority.

The project, co-ordinated by one of the Authors [1], involves an international group of researchers and had the aim of assessing the physical and structural decay of the Church and all its components (roof, masonry walls, columns, plasters, mosaics and paintings). The ultimate aim was to provide specific recommendations and guidelines for appropriate restoration and consolidation interventions.

The preliminary studies included historic and archaeological research [2], analysis of the mosaics [3],

non-destructive tests on stones and masonry [4], in situ and lab tests on wooden elements [5–7] and an initial study of the seismic vulnerability of the Church [8]. This yielded several indications as to the most suitable practical consolidation interventions, as well as some technical recommendations for the restorers who would subsequently be engaged to carry out the practical phase of the project [9].

An example of how the mechanical behaviour of buildings under seismic loads can be studied was provided by Mele et al. [10], who developed a 3D finite element (FE) model for static and dynamic analysis of a basilica. This breaks the structure down into a number of 2D macro-elements, which can subsequently be studied by non-linear analysis.

Like many basilicas of the early Christian period, the Church of the Nativity rests on four colonnades placed at both sides of the nave (Fig. 1). The vulnerability of classical columns to dynamic excitations has been investigated by Papalau [11] using Finite Element numerical models. Lagomarsino and Podestà [12], on the other hand (following the 1997 earthquake that struck some regions of central Italy), described a methodology for assessing seismic damage to ancient churches by means of 18 geometric and technological indicators. However, the latter approach is more useful from an urban-planning perspective, as the indicators defined are strictly related to the specific areas taken into account.

In another study, Mallardo et al. [13] analysed the seismic behaviour of an important Renaissance palace in Ferrara (Italy) using 2D and 3D FE models; they show that 3D structural analysis of the entire building is only significant when a good level of interlocking among structural elements is guaranteed. If such connections are not reliable, as in some parts of the Church of the Nativity, it is advisable instead to perform 2D analyses on smaller portions

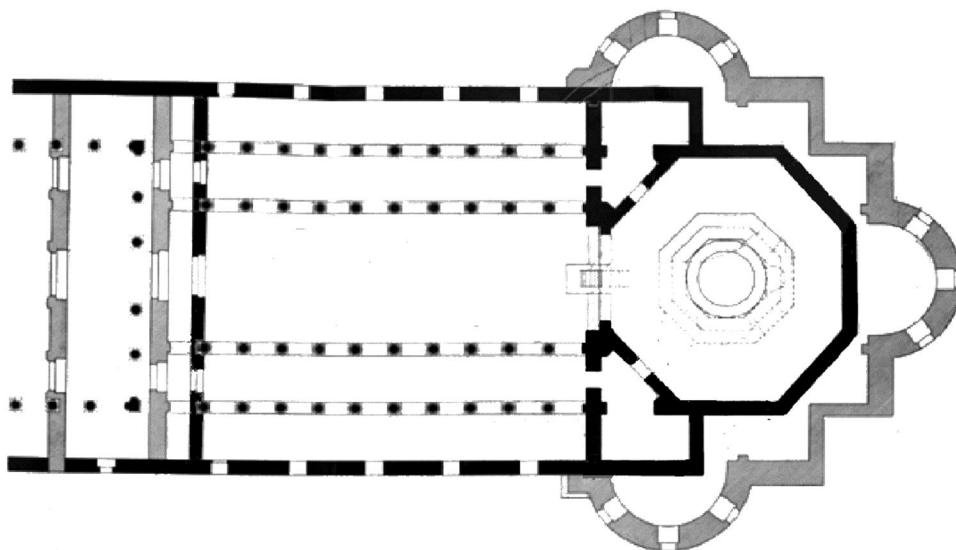
of the building that may be affected by local collapse mechanisms.

The present state of damage in the narthex of the Church of the Nativity, likely due to major seismic activity in the past, has recently been reproduced by means of non-linear dynamic analyses by Milani et al. [14]. As it involves several spectrum-compatible acceleration–time histories of the base of the structure, the proposed method is rather time consuming, but is much more accurate and reliable than other approaches. This is because of its capability to identify in- and out-of-plane horizontal displacements, as well as local and global failure mechanisms. Moreover, 3D FE modelling takes into account geometrical (large displacements) and material (elastic–plastic behaviour and damage) non-linearity.

The purpose of this paper, however, is not to address the many numerical problems related to the non-linear analysis of masonry structures, but rather to propose an innovative technique for consolidating a wall of the Church of the Nativity, whose evident seismic vulnerability is the cause of significant concern at the present time. Although retrofitting techniques based on sprayed cementitious composites, with or without additional wire mesh, have been developed for unreinforced masonry walls [15], for a building of such historic and religious importance the alteration of existing surfaces is prohibited.

Section 2 of this paper contains a short description of the main architectural features of the Church as a whole, and the wall under investigation in particular, while Sect. 3 describes the local seismicity characteristics and parameters used to plot the elastic response spectrum. The mechanical properties of the main building materials of the Church are presented in Sect. 4, and then used, in Sect. 5, in 3D modal analysis of the Church as a whole. This enabled identification of the parts of the Church with the most

Fig. 1 The Basilica according to Bagatti's re-construction. Black Constantine's Church. Grey Justinian's Church



significant modes of vibration and, therefore, the greatest seismic vulnerability. Among these is the wall examined in this paper, which is then analysed in detail in Sect. 6, according to [19], as a macro-element subject to the collapse mechanism suggested by the actual boundary constraint conditions. With reference to this collapse mechanism, an innovative consolidation technique is presented in Sect. 7.

This consists of a tension-structure system, which, unusually, acts in the horizontal, rather than vertical, plane. Moreover, it possesses all the structural characteristics necessary to meet the main Restoration Charter requirements, such as reversibility, lightness and non-invasiveness. In Sect. 7, the resultant horizontal loads transferred by the tension-structure system to the wall are computed as forces in equilibrium with the equivalent seismic load, and in Sect. 8 the linear elastic FE analysis carried out on the wall is described. This analysis took into account the boundary constraints consistent with the identified collapse mechanism, and was designed to evaluate the pre-tensions in the cables corresponding to maximum horizontal displacements lower than those admissible. The wall was then analysed under all applied loads computed, i.e. own weight, seismic loads, and cable pre-tensions, acting simultaneously. Due to a lack of reliable local regulations, all analyses were carried out with reference to the Italian regulations; all checks on the horizontal displacements gave satisfactory results.

2 Architectural Features

According to the most recent studies [2], the Church of the Nativity was completely re-built upon the remains of Constantine's previous Church (fifth century AD) in the sixth

century AD by Emperor Justinian. Its longitudinal body, which is slightly longer than the previous footprint (Fig. 1), consists of a nave with four flanking aisles and four colonnades, two on each side. A transept and an apse took the place of the original octagonal structure built above the main Grotto, which was visible from a hole placed in the centre of the octagon. Detailed archaeological reports can be found in the books of Hamilton [16] and Harvey [17], as well as in the comprehensive research carried out over many years by Bagatti [18].

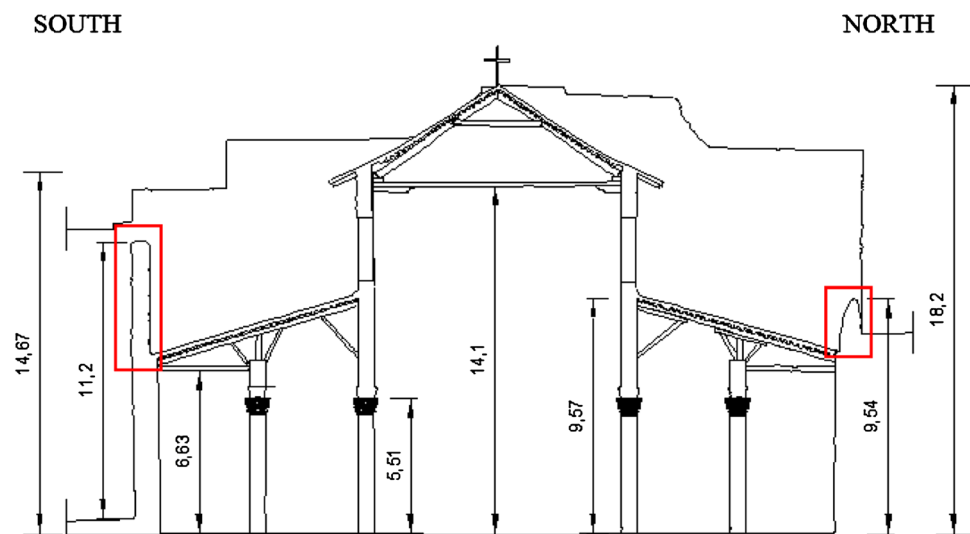
During the Crusades (twelfth century AD), the Church underwent several transformations, mainly involving the roof structure of the narthex. Some additional perimeter walls were also raised over the existing ones, probably for defensive purposes. In particular, two additional walls were built above the external walls of the longitudinal body for a length of about 28 m—one to the north, which was 1.50 m high, and the other to the south, 4.50 m high. (Fig. 2).

Careful stratigraphic analysis of the addition above the south wall (Fig. 3) has evidenced that the wall in this section was thinner, the stones used were smaller, and there was a change in the way that these stones were worked and finished. It also shows that some stones were taken from other parts of the Church, like, for instance, a long block of pink limestone, which bears several marks and inscriptions (circled in Fig. 3).

It is worth noting that this wall was simply built butting up against the pre-existing orthogonal ones, although there are some decorative stones, visibly protruding from the transept wall on both sides of the basilica (Fig. 4), which were probably placed to improve the connection. However, these stones did not serve to greatly strengthen the joint.

Moreover, the considerable length of this wall and the absence of intermediate retainers make the wall highly vulnerable in the event of seismic activity. If the wall did

Fig. 2 Additional walls built during the Crusades—view from the apse



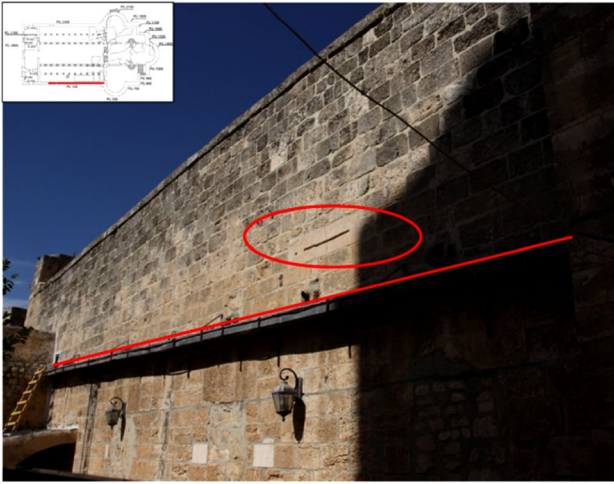


Fig. 3 View of the additional south wall

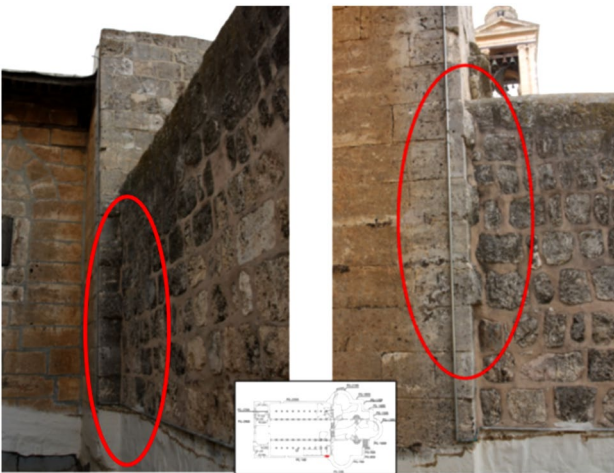


Fig. 4 Connections between the additional wall and the pre-existing orthogonal ones

collapse, it would doubtlessly endanger the safety of many visitors, as well as damaging the recently restored roof over the aisles. To avert such potential damage, the Authors set out to design a consolidation system that would meet all the strength and safety requirements and main principles of restoration, such as reversibility, lightness and non-invasiveness.

3 Seismicity of the Site

Bethlehem is located between two areas of medium–low seismicity, one to the west and one to the east side. It is situated close to the fault line separating the African and

Arabian tectonic plates (Fig. 5), and has, in the past, been affected by several minor and major earthquakes with epicentres in the surrounding areas.

As the laws and available data concerning the site seismicity are insufficient for conducting an accurate seismic analysis of the Church, the Authors referred instead to the Italian regulations and the more comprehensive data on seismic activity in Italy, another earthquake-prone region. Naturally, this involved some corrective measures to adapt the Italian data to the local context, but the Authors endeavoured to identify a comparable site on the basis of the seismic zoning of the Palestinian Territory and the Italian Technical Standards for Constructions NTC [19]. Indeed, the Italian site selected had the same ground acceleration ($a_g = 0.15$ g) and the same altitude (600 m) as Bethlehem, and a comparable return period of 475 years. The longitude and latitude of an “equivalent” point on the Italian seismic zoning map was then determined to define the corresponding response spectrum.

As in [19], and as prescribed for a dynamic linear analysis of existing buildings, a behaviour factor within the range 1.5–3 ($q=2.0$) was chosen with reference to the already available technical data, and the so-called life limit state (LLS) was assumed as the limit state, according to which, “in consequence of an earthquake, the building may undergo a significant loss of stiffness towards horizontal actions, although preserving part of the original stiffness and resistance to vertical actions, as well as a reasonable safety margin towards damages due to horizontal seismic actions”.

Also as in [19], a return period $T_R = 475$ years was defined, and the reference period V_R for the seismic action was assumed as follows:

$$V_R = V_N \times C_U = 100 \times 2.00 = 200 \text{ years}, \quad (1)$$

where $V_N = 100$ years is the nominal life of a structure, i.e. the number of years during which a structure with strategic importance can perform its functions, provided that it receives proper maintenance, C_U is a use coefficient that depends on the particular functions of a prescribed building; in the case of buildings with high historic and cultural relevance, $C_U = 2$.

Due to a lack of detailed local geological data, the elastic response spectrum was plotted using a simplified approach described in [19]. In particular, with reference to Subsoil Category B (soft rock and very thick layers of coarse- or fine-grained soils) and Topographic Category T1 (flat land, slopes and isolated hills with an average inclination $i \leq 15^\circ$), the following parameters were defined:

- the stratigraphic amplification factor S_S in the range $1.00 \leq 1.70 - 0.60 \times F_0 \times \frac{a_g}{g} \leq 1.50$,

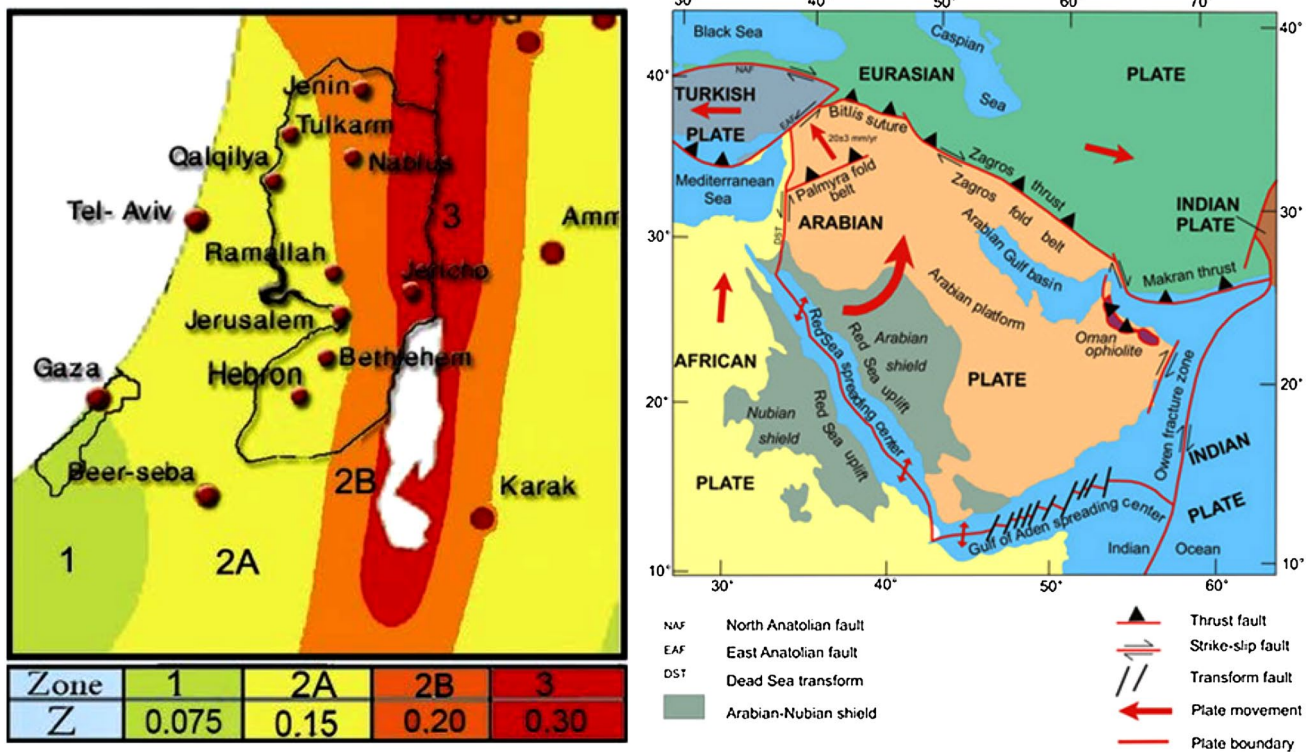


Fig. 5 Seismic map of the area and fault line between the African and Arabian plates

- the coefficient $C_c = 1.10 \times (T_c^*)^{-0.2}$, which depends on the subsoil category;
- the topographic amplification factor $ST=1$, which depends on the topographic location of the building

where a_g is the maximum horizontal ground acceleration, g the acceleration due to gravity, F_0 the maximum value of the amplification factor of the spectrum, and T_c^* the period at the beginning of the constant interval of the diagram.

All these data and the geographical coordinates of the Italian equivalent site were entered into the computer code SPETTRI NTC, ver. 1.0.3, published on the Italian website of the Higher Council of Public Works [20]. The reference elastic spectrum (S_e), the design spectrum in the vertical component ($S_{d,v}$) and horizontal component ($S_{d,o}$) were obtained according to the procedure described in [19], as shown in Fig. 6, which yielded the following values:

- $a_g = 0.253 g$
- $F_0 = 2.550$
- $T_c^* = 0.363$

In Sect. 5, these seismic inputs will be used as part of the 3D modal analysis to identify the most vulnerable

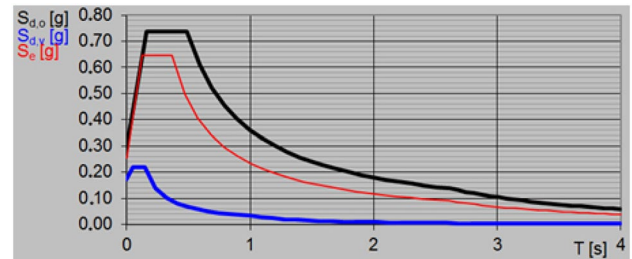


Fig. 6 Elastic and design spectra obtained by means of the computer code SPETTRI NTC

parts of the Church, among which is the south wall, which the proposed intervention is designed to reinforce.

4 Mechanical Properties of the Material Components of the Church

A number of onsite tests have been carried out on the structural components of the Church since the beginning of the survey campaign in 2010. Sonic, ultrasonic, radar, thermographic and infrared tests have been performed on masonry walls and stone columns, and stone specimens similar to those used in the Church construction have been subjected

Table 1 Masonry constructed using squared stones (sixth century AD)

f_m (MPa)	t_d (MPa)	E (MPa)	G (MPa)
4.66	0.089	1429	460.75

f_m the compressive strength, t_d the shear strength, E the Young's modulus, and G the shear modulus

Table 2 Masonry constructed using roughly cut stones (Crusader period)

f_m (MPa)	t_d (MPa)	E (MPa)	G (MPa)
3.49	0.067	868.38	147.25

f_m the compressive strength, t_d the shear strength, E the Young's modulus, and G the shear modulus

Table 3 Masonry constructed using loose material (Crusader period)

f_m (MPa)	t_d (MPa)	E (MPa)	G (MPa)
1.01	0.02	456.75	147.25

f_m the compressive strength, t_d the shear strength, E the Young's modulus, and G the shear modulus

to material analysis [4]. The results obtained show quite high-average values for the masonry density and the compressive strength of the masonry walls of the nave and aisles. Indeed, these were built in the sixth century AD and are characterized by large, well-cut stones with very thin and regular mortar joints.

Very different are the characteristics of the walls added in later, Crusader time; these are made of roughly cut stones, and the mortar between them is thick and irregular.

For these later additions it was deemed more appropriate to use the results of a materials survey recently carried out on the narthex, whose perimeter walls, coeval with the Church, bear cross vaults from the Crusader period and possess very similar material characteristics to those of the wall that is considered in this analysis. In the narthex the following three types of masonry were identified.

The first type of masonry (Table 1) is the one used in the construction of the perimeter walls of the narthex and the Church itself; the second (Table 2) is the one used to construct some specific narthex components—like the internal walls—added in the Crusader time, the groins of the cross vaults, and the external additions; the third (Table 3) is the one used to construct the vaults themselves. It is worth noting that owing to the limited information available on the building characteristics, all values reported in Tables 1, 2 and 3 were obtained, according to [21], by dividing the actual surveyed values by a proper

Table 4 Mechanical characteristics of the columns

E (MPa)	ν (-)	w (KN/m ³)
59,259	0.2	20

Table 5 Mechanical characteristics of the roof trusses

E (MPa)	ν (-)	w (KN/m ³)
9259	0.15	7.05

confidence factor F_c , here corresponding to the lowest level of knowledge, the so-called confidence level LC1, and given by:

$$F_c = 1 + \sum_{k=1}^4 F_{ck} \quad (2)$$

where $F_{ck} \geq 0$ increases in line with the decreasing accuracy of the data.

In particular, $F_c = 1.35$ for the following F_{ck} values:

- $F_{c1} = 1$: complete geometric survey.
- $F_{c2} = 0.12$: hypotheses on the building phases based on a limited material survey associated with some historical documentation.
- $F_{c3} = 0.12$: material properties obtained from available data.
- $F_{c4} = 0.06$: limited investigations on subsoil and foundations in the absence of more detailed data.

The Poisson coefficient $\nu = 0.2$ and the average specific masonry weight $w = 18 \text{ KN/m}^3$ were taken from the technical literature.

Although processed in different ways, the stone used in the construction of the church is all meleke, also transliterated as melekeh or malaki, a type of white, coarsely crystalline, thickly bedded limestone that is very common in the Judean Hills of Israel and the West Bank, and has been used in the local traditional architecture since ancient times. As for the other components, their material properties were determined in a previous survey campaign, carried out in 2010. In particular, the mechanical characteristics of the columns (Table 4), made of local red crystalline limestone, were determined in part by means of sonic and ultrasonic onsite tests [4], and partially extrapolated from the technical literature.

The material properties of the wooden roof trusses (Table 5), mostly made out of larch and oak, have been described in detail in [5].

The reduced Young's moduli of both the columns and the wooden elements were obtained using the same confidence factor used for the masonry (F_c). These material

properties were then applied to the FE model used in the 3D modal analysis, as described in the following section.

5 3D Modal Analysis

Modal analysis of the entire Church was necessary to predict the global response of the building to external actions, and to identify the parts with the greatest seismic vulnerability, as well as to highlight possible local kinematic behaviours that would be useful in the detailed analysis of local collapse mechanisms.

As in [19], this analysis was carried out using a 3D linear elastic FE model and Straus7 software [22], and the results are reported in terms of natural frequencies and mass percentages activated by each mode. This model was constructed on the basis of a laser scanner geometric survey, and some simplifying assumptions on several structural components. In particular, the cross vaults of the

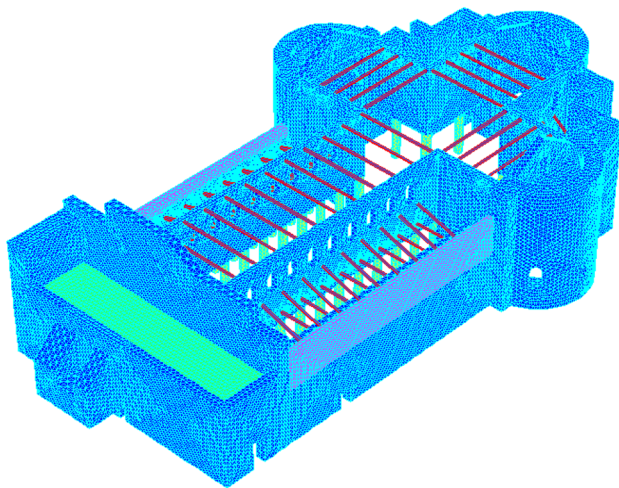
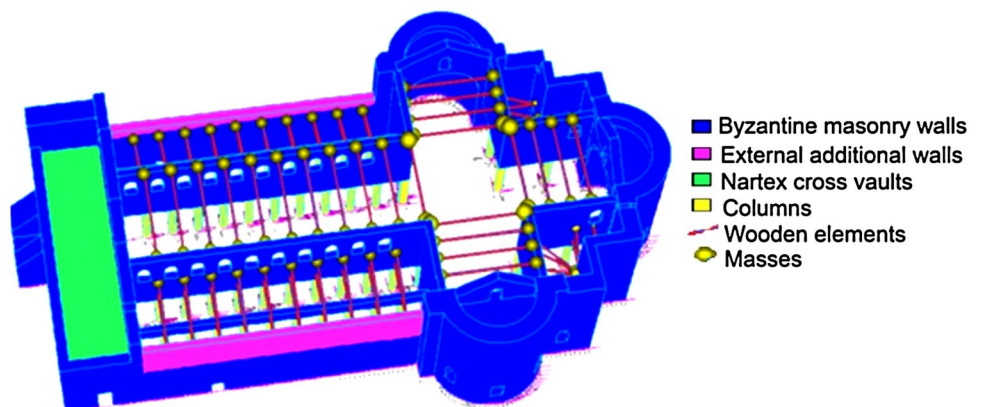


Fig. 7 3D discretized linear elastic FE model developed by Straus7–103 beams elements, 375,431 tetrahedral brick elements, 92,256 nodes

Fig. 8 Materials, masses and constraints of the 3D FE model



narthex are represented with identical geometric characteristics, despite some slight differences in height, and the main roof trusses are represented in the model only by their tie beams and the vertical loads they transfer to the walls. Moreover, some constraints were applied to several parts of the external surface to simulate the presence of the existing adjacent buildings.

The model was discretized by means of 103 beams elements, 375,431 tetrahedral brick elements and 92,256 nodes, with mesh size 50 cm everywhere except in the areas where higher stress concentrations were expected (Fig. 7).

Figure 8 shows the variety of the component materials, i.e. Byzantine masonry walls (Table 1), narthex cross vaults (Table 3), external additional walls (Table 2), columns (Table 4), and wooden elements (Table 5).

It also shows the masses concentrated at both ends of each truss and the boundary constraints.

For the sake of brevity, only the vibration modes activating the highest mass percentages are shown in Fig. 9.

Table 6 reports the frequency, total modal mass, and percentage values of mass activated in the x -, y - and z -directions, (i.e. longitudinal, transverse and vertical) respectively, for the first ten vibration modes.

This global analysis shows that the structure is mainly characterized by local modes, particularly in the longitudinal walls of the nave and aisles (Fig. 9a, b, d), and in the tympanum of the façade (Fig. 9c). Other local but less significant modes are clearly visible in the apse and adjacent corners. As expected in this type of building, the compactness of the whole structure results in rather low values for activated mass percentage and high values for frequency.

The dynamic behaviour of the Church is summarized, as previously performed by Brandonisio et al. [23] and Milani et al. [24–26], in Fig. 10a, b, where the modal participating mass ratios (M_{eff}) of the first ten modes analysed in both transverse and longitudinal directions are plotted as a function of the vibration period (T). It is very clear that almost all vibration modes, except modes 4 and 9 in the

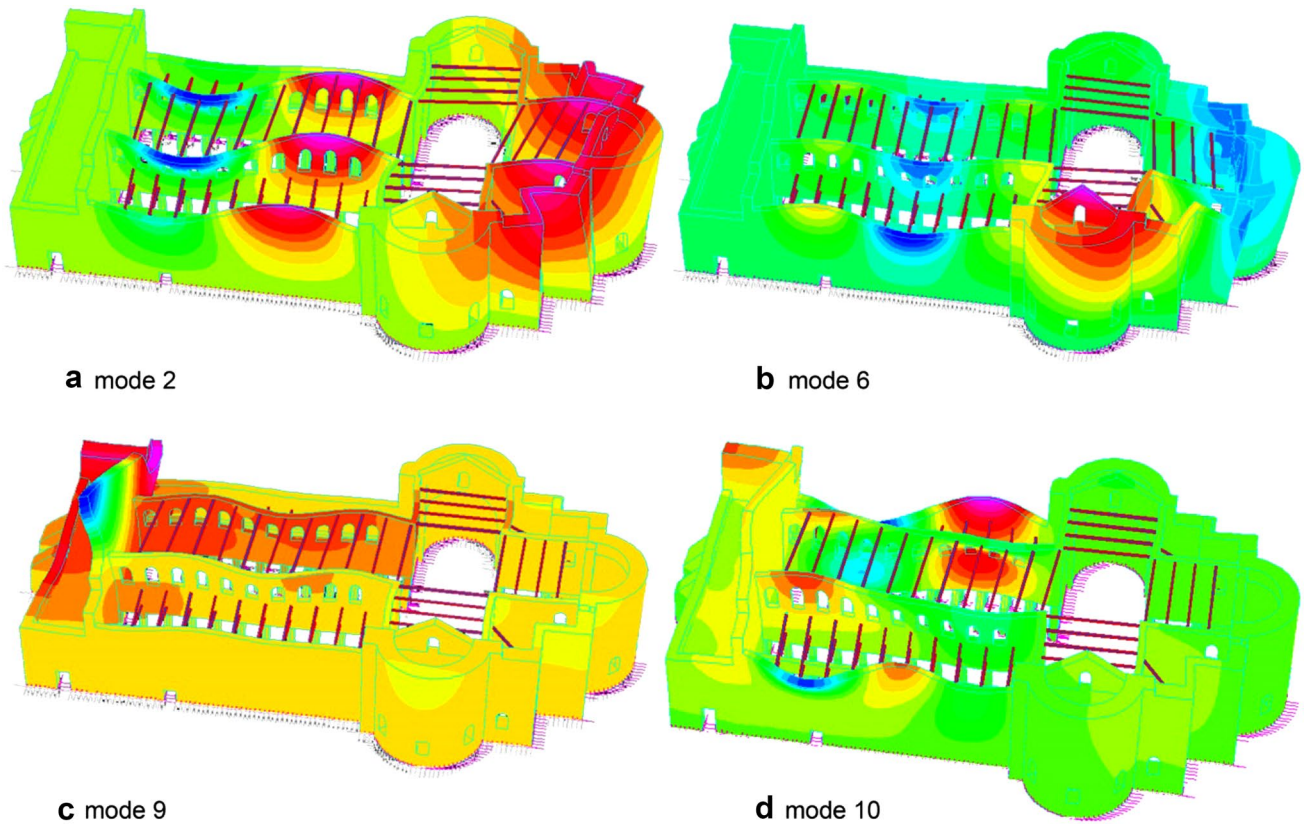


Fig. 9 Modes activating the highest mass percentages

Table 6 Vibration modes

Mode	Frequency (Hz)	Modal mass (KN)	Mass, x (%)	Mass, y (%)	Mass, z (%)
1	2.669	831.70	0.000	5.786	0.000
2	4.106	582.30	12.275	0.209	0.007
3	4.279	3995.00	6.764	4.616	0.013
4	4.525	532.80	0.032	4.727	0.010
5	5.147	639.60	0.019	10.946	0.017
6	5.512	7535.00	13.506	6.493	0.000
7	5.625	2515.00	5.706	0.010	0.021
8	5.698	2247.00	3.159	2.237	0.002
9	6.367	1301.00	14.620	1.065	0.047
10	6.900	1330.00	0.012	11.953	0.031
TOT	–	–	56.093	48.042	0.148

The bold values refer to the modes shown in Fig. 9

longitudinal direction and mode 7 in the transversal direction, have a modal participating mass ratio (M_{eff}) of less than 10%. This means that the dynamic response of the Church is strongly affected by the local behaviour of the macro-elements.

By comparing Fig. 10a, b with Fig. 6, it can also be observed that the vibration modes with the higher participating mass ratios correspond to very low spectral

acceleration values with respect to peak values; this justifies the assumption of rather low values for the base shear forces. For the modes characterized by the largest values of participating mass, a 3D view of the corresponding deformed configurations is also provided. In particular, Fig. 10a shows modes mainly involving vibrations in the longitudinal direction of the church, while Fig. 10b refers to the modes in the transverse direction. From the data shown

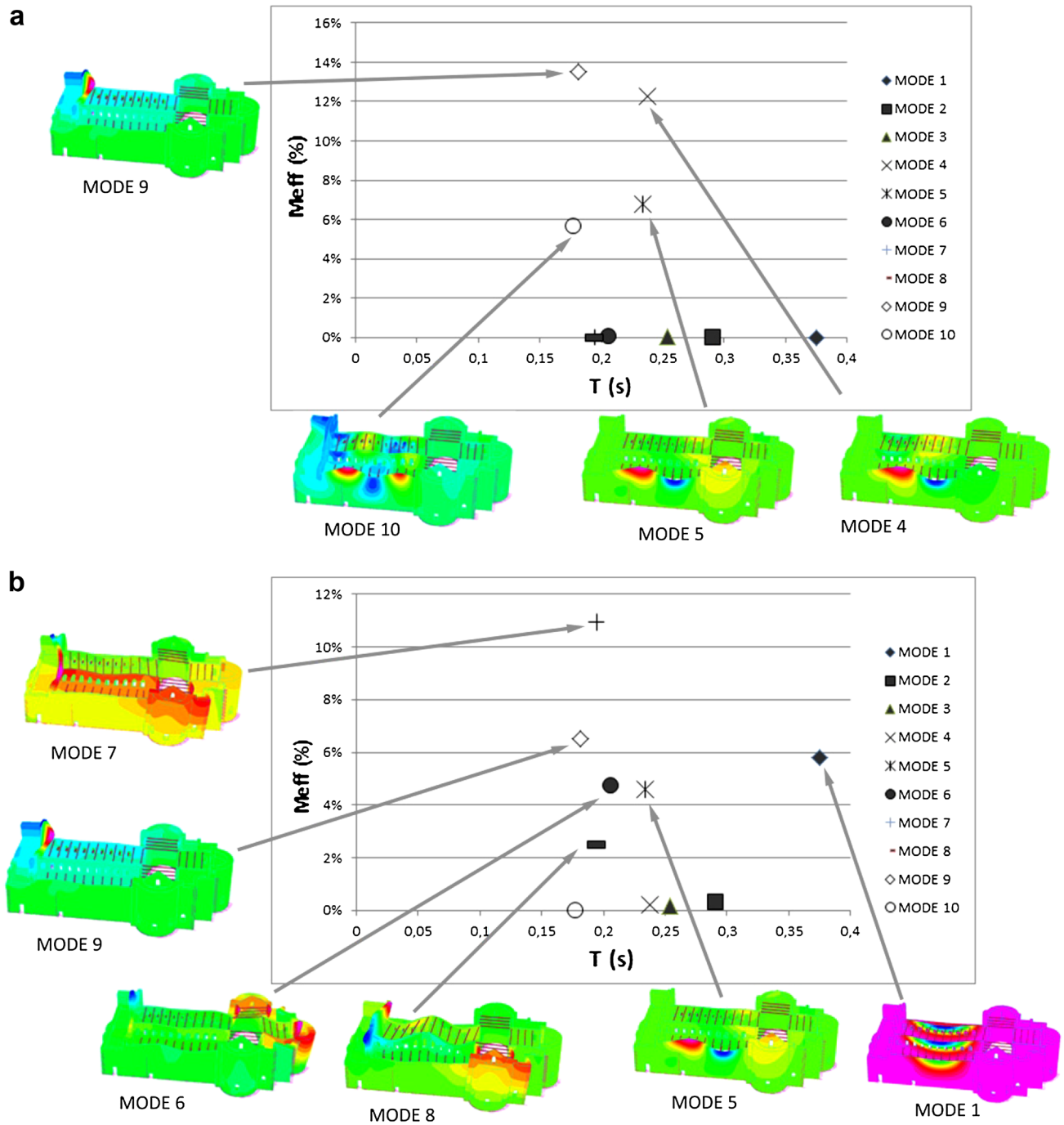


Fig. 10 Distribution of the first ten modal shapes for the earthquake acting in longitudinal (a) and transverse directions (b)

in Fig. 10b it is possible to deduce that the first mode associated with a non-negligible participating mass is mode 1, namely the first out-of-plane mode of the longitudinal walls and internal colonnades, whereas the higher modes in the

same direction mainly involve deformations of the apse and the transept. In the longitudinal direction, the vibration modes mainly involve deformation of the external walls of the aisles.

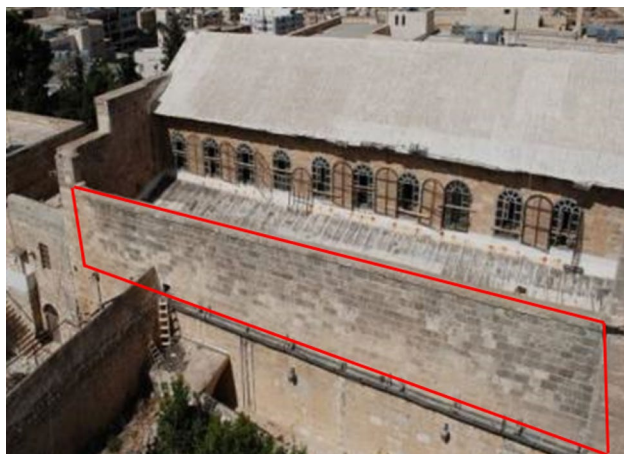


Fig. 11 View of the south wall addition

6 The Collapse Mechanisms of the Additional South Wall

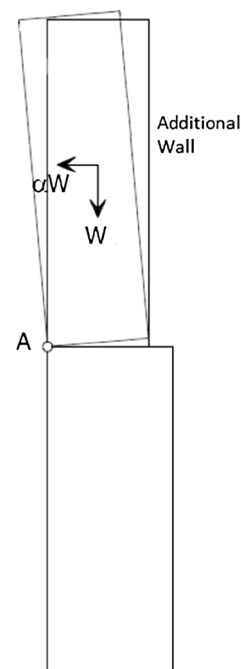
The results of the 3D modal analysis clearly show the parts of the Church where collapse mechanisms are more likely to occur, namely the tympanum and the Crusade-era wall additions on both the north and south sides. According to the most recent studies on masonry structures, and the prevailing trend in the analysis of such structures, these parts might be better analysed as macro-elements in a local linear kinematic analysis.

All checks carried out on the tympanum and the north wall yielded satisfactory results, as might be expected from their reduced dimensions, especially in height. The biggest concern was for the south wall, which is 4.5 m high, 28 m long and 70 cm thick, without any intermediate retainer (Fig. 11). If this wall should collapse, it could seriously endanger the safety of visitors, and cause considerable damage to the roof of the southern aisle, even though this has recently been restored.

As this wall was added to the pre-existing Byzantine structure, its connections with the underlying wall of the aisle and the two orthogonal walls at both ends cannot fully be reliable upon, and many uncertainties exist regarding their effectiveness. In fact, the stones of this wall are simply butted against the other walls, with no evidence of strong connections able to guarantee resistance against horizontal loads. Not even the presence of some decorative stones protruding from the external surface of the transept (Fig. 4) is able to guarantee an effective link.

Furthermore, the entire wall addition simply rests on the top of the pre-existing south wall, which, however, was recently restored and firmly connected to the roof by means of threaded steel bars. It is, therefore, reasonable to assume that the additional wall simply rests on the aisle wall, being

Fig. 12 Simple overturning collapse mechanism of the additional wall around a side of its base



unconstrained at both vertical sides and, therefore, likely to overturn around one side of its base in the presence of specific horizontal loads (Fig. 12). The hinge A is at 7.4 m from the ground, at the base of the additional wall. The macro-element considered in the standard linear kinematic analysis is 1 m long.

Both checks on safety and the limit state of damage, carried out according to [27] and using Mc4 Loc Software [28], which was specifically designed for analysis of local mechanisms, yielded unsatisfactory results.

7 Structural Consolidation of the South Wall Addition

Owing to the peculiarity of the building, the structure used to consolidate the south wall has to be non-invasive, light, as reversible as possible, and able to guarantee the stability of the wall in the presence of the predicted seismic actions. It seemed that all these requirements could be fulfilled by horizontal tension structures characterized by cables with opposing curvatures. These would bear horizontal loads, orthogonal to the wall and acting both inwards and outwards. Similar, but not identical, consolidation techniques can be found in some Italian technical recommendations for consolidating masonry buildings in seismic areas. In such cases, a net of cables, resting on the floor, is linked to the perimeter walls so as to prevent their relative horizontal displacements and the floor slipping off [29]. Such a system, resting on a plane and with only one working cable, has also been used to limit the relative horizontal

Fig. 13 The two horizontal tension-structure systems and dimensions of the anchorage tube

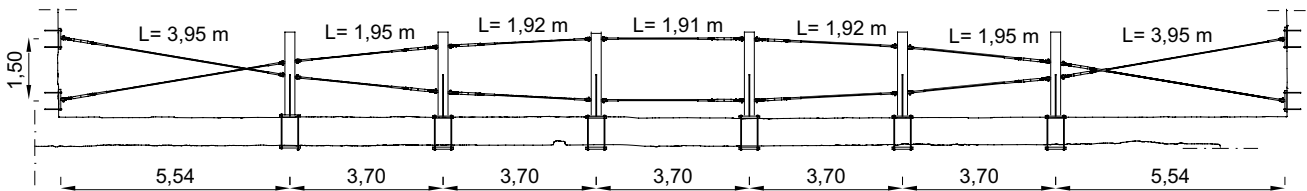
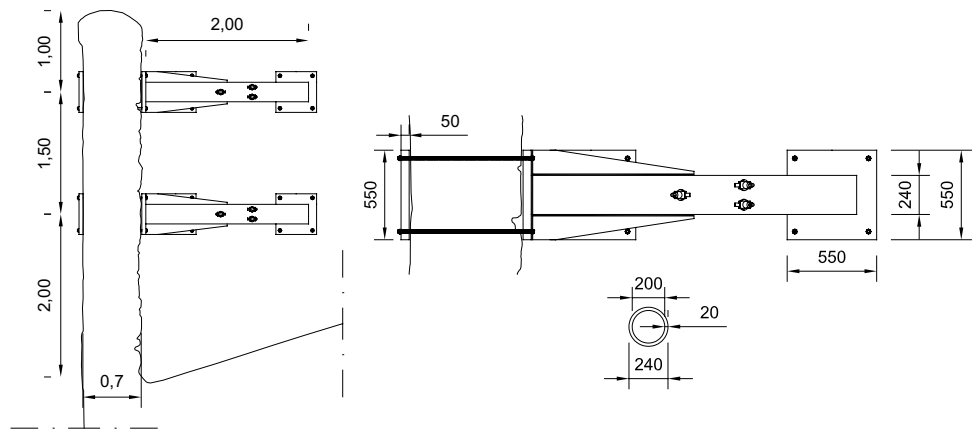


Fig. 14 Horizontal view of each tension-structure system

Fig. 15 Axonometric view of both tension-structure systems

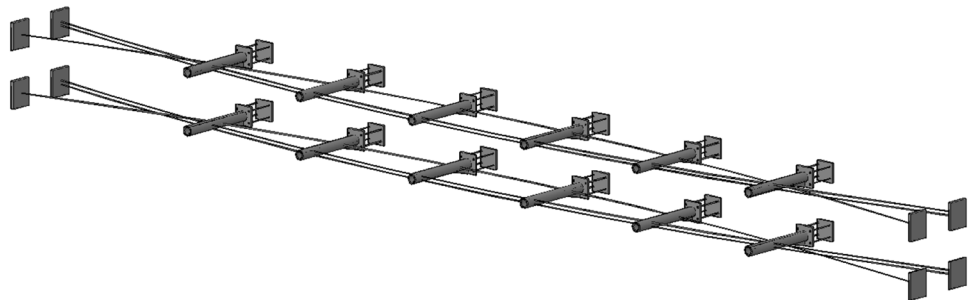


Table 7 Geometric characteristics of the cables

Assembling	Description	Cable diameter (mm)	Weight (KN/m)	Wire diameter (mm)	Ultimate tensile stress	
					1470 N/mm ² (KN)	1570 N/mm ² (KN)
 6x(14+(7+7)+7+1) + IWRC		20	0.0167	1.14	–	221

displacements of the masonry pillars in the Cathedral of Cremona (Italy) [30].

The concept behind such structures and how they behave are clearly illustrated in the following figures.

Two tension-structure systems were designed to fit at 2.00 and 3.5 m from the base of the wall addition (Fig. 13). Each consists of three steel cables, one with the convex part facing outwards, the other two, placed symmetrically

Table 8 Mechanical characteristics of the cables

Physical properties	
Density	79 (KN/m ³)
Young's modulus	200,000 (MPa)
Thermal conductance	15 (W/m °C)
Thermal resistance	500 (J/kg °C)
Electrical resistance	0.73 (μ Ωm)
Mechanical properties	
Yield stress	280–290 (MPa)
Ultimate strength	570–590 (MPa)

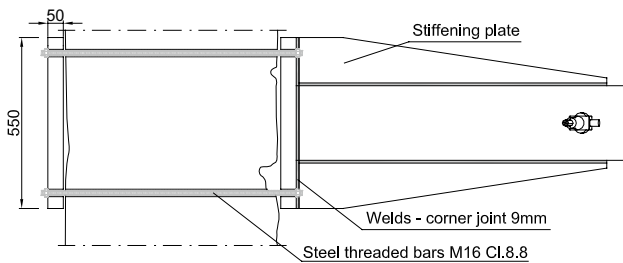


Fig. 16 How the plates are anchored to the wall

with respect to the mid-plane of the whole system, with the convex part facing inwards (Figs. 14, 15).

The cables, made out of INOX AISI 316 steel, possess the geometric and mechanical characteristics shown in Tables 7 and 8, respectively.

The cables are connected to the wall by means of six horizontal tubes of circular cross section set apart from one another, from the orthogonal walls and from the base of the wall, as shown in Figs. 13 and 14. The external diameter, thickness and length of the tubes are shown in Fig. 13.

Each tube is anchored to the wall by means of two 50-mm-thick square steel plates measuring 550 × 550 mm. These are placed on both sides of the wall

and connected to one another by four-threaded steel bars of diameter 16 mm (Fig. 16).

The behaviour of the cables during an earthquake will depend upon the direction of the forces exerted upon them; the horizontal bars that connect them to the wall can be either compressed (Fig. 17) or stretched (Fig. 18).

Figure 19 shows the connection of the outwardly convex cable with the tubes and wall anchorage plate.

The same type of connection is also used for the cables with inward convexity.

A pre-tension value, computed in the following section, is given to all cables, so as to strengthen the wall against seismic assault, and also to prevent such cables assuming a catenary shape in the vertical plane under their own weight. The cables, actually made out of a set of cables stretched between two consecutive tubes (Fig. 19), are fixed to the orthogonal walls of the Church façade and transept by means of eight square steel plates (the same dimensions as the others), four on each side (Figs. 14, 15), and threaded steel bars, four for each plate, of diameter 16 mm (Fig. 20).

The steel tubes and plates employed are made out of galvanized steel S355, which has the material properties shown in Table 9.

Figure 21 shows the tensioner in its limit configurations.

The resultant loads transferred by the tension-structure system to the wall were computed as the loads able to prevent the overturning of the wall under the wall's own weight and the equivalent seismic load. For this purpose, a portion of wall 3.7 m long and 4.5 m high, incorporating a set of two tubes placed one above the other, was considered, subject to its own weight, proportional seismic action, and the horizontal loads transferred from the cables to the wall through the horizontal tubes (Fig. 22).

The rotation of the wall was designed to occur around the cylindrical hinge positioned along one edge of the base and represented by point A in Fig. 22 where

- $W = \gamma \times b \times h \times l = 209.8$ KN is the own weight of the masonry portion;

Fig. 17 Inward-oriented seismic loads: tension in the two cables with inward convexity—compression in the tubes

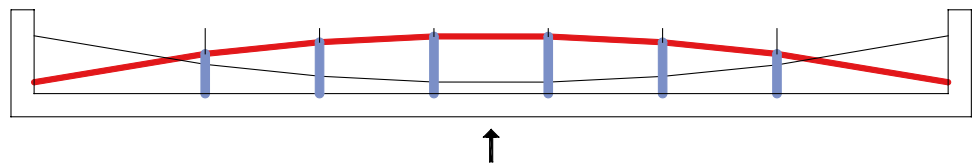
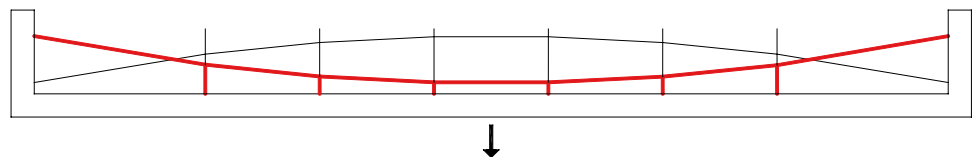


Fig. 18 Outward-oriented seismic loads; tension in the cable with outward convexity—compression in the tubes



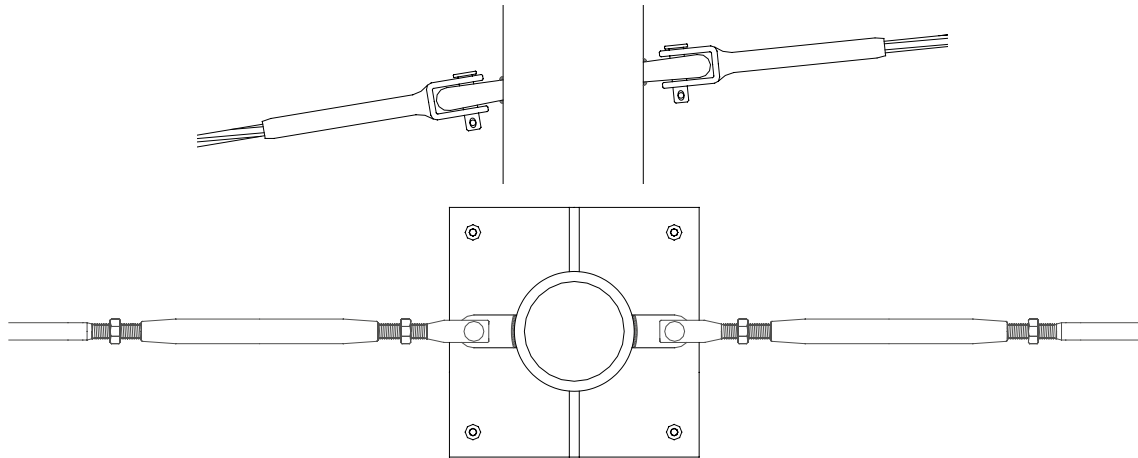


Fig. 19 Outward-convexity cable and its connection via tubes and anchorage plate

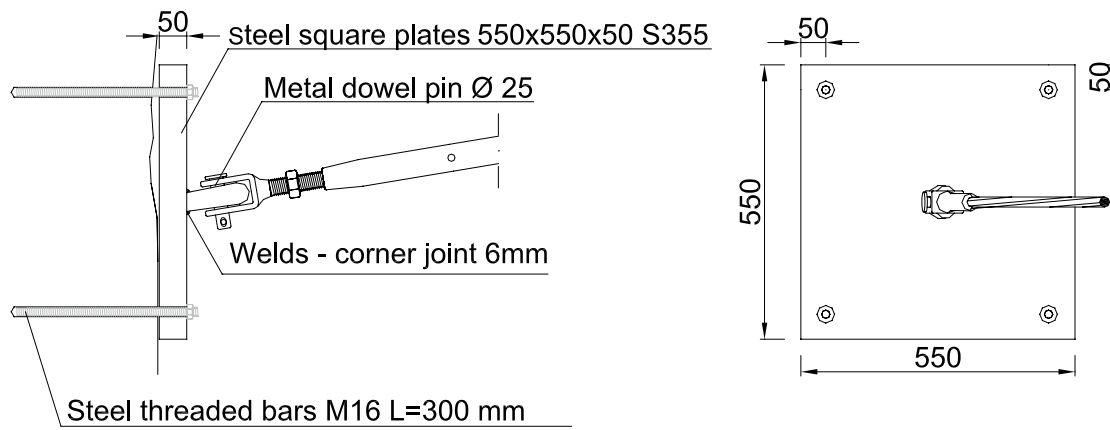


Fig. 20 Anchorage of a cable to an orthogonal wall

Table 9 Material properties of galvanized S355 steel

Galvanized S355 steel	
Young's modulus	210,000 (MPa)
Poisson coefficient	0.3 (-)
Density	78.5 (KN/m ³)
Yield stress	510 (MPa)
Ultimate stress	355 (MPa)

- T_1 and T_2 , placed in correspondence with the two tension structures, are the stabilizing loads;
- $\alpha_0 \times W$ is the equivalent seismic load;
- $\alpha_0 = 0.293$ is the collapse multiplier satisfying the ultimate limit state linear control performed according to [20].

By assuming T_1 and T_2 as proportional to their distances from the base it is possible to write:

$$T_2 = \frac{h_2}{h_1} T_1 = \frac{2.00}{3.50} T_1, \quad (3)$$

and the equilibrium around the hinge provides

$$M_s = W\left(\frac{t}{2}\right) + T_1 h_1 + T_2 h_2 = M_o = \alpha_0 W\left(\frac{h}{2}\right), \quad (4)$$

where M_s is the stabilizing moment and M_o is the overturning moment. Consequently:

$$T_1 = 15.00 \text{ KN and } T_2 = 8.75 \text{ KN.}$$

For the sake of simplicity, a single value for such concentrated loads, $T = 15.00 \text{ KN}$, was assumed for the tension structures at both levels. However, the authors believe that the ground acceleration defined for Bethlehem, as described in Sect. 2, is unreliable, as Bethlehem

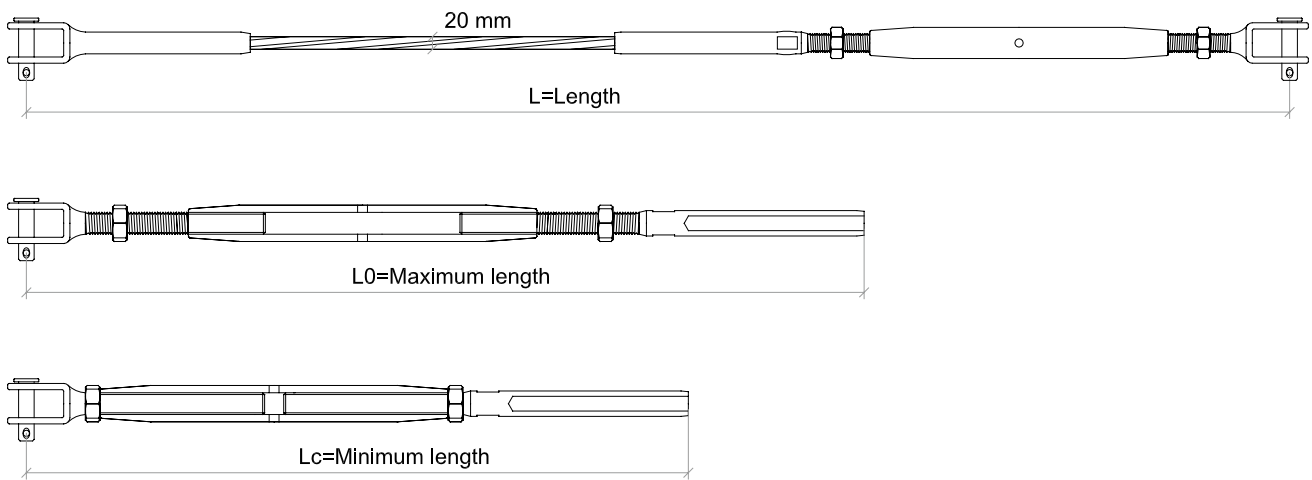


Fig. 21 Tensioner limit configurations

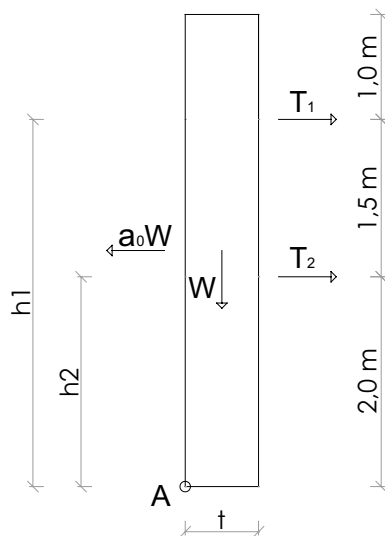


Fig. 22 Loads acting on the walls in the case of an earthquake

is very close to the Anatolian fault, which has caused a lot of serious earthquakes recently and in the past.

For this reason, the computed value was multiplied by a 1.5 safety factor. Consequently, the value of the concentrated loads in correspondence with both tension-structure systems becomes 22.5 KN. Such loads, assumed in equilibrium with an obviously increased seismic load $\alpha_0 W$, will be the seismic loads applied to the FE model, described in the next section, in correspondence with the tubes of the tension-structure system.

It is worth noting at this point that the wall consists of two outer walls made of fairly regular stones, and an inner filling of poorer material. For this reason, it would not be advisable to hide the anchor steel plates within the masonry, as its resistant cross section would be considerably reduced,

as would the strength of the entire wall. However, the wall overlooks an inner courtyard that is not accessible to ordinary visitors (Fig. 23) and, therefore, the plates in this system remain visible only to the members of the religious communities who manage the place (Fig. 24).

Furthermore, it would be possible to paint the plates with protective paint of a similar colour to the wall. In any case (Fig. 24), the entire system of tension structures remains completely invisible to an observer from below. It is also fairly reversible as the anchorage to the walls is obtained using bolted steel bars that can easily be removed.

8 FE Analysis of the Consolidated Wall

The computations were carried out using the FE code Straus7 [22] in a linear elastic analysis. Further checks with non-linear analysis will be performed at a later stage of the research. For the purposes of the linear analysis, the wall was discretized into 52,272 tetrahedral brick elements, with 11,638 nodes and a mesh size of 20 cm, while the steel tubes and cables were modelled by beam elements. Although the cables could have been modelled by cable elements, the pre-tension values necessary to provide adequate resistance to the seismic loads—70 and 50 KN, as shown later in this section—are far higher than those needed to keep the cables straight under their own weight. Furthermore, these loads would be sufficient to keep the cables in a constant state of tension under the prescribed loads. For this reason, even the cables were modelled by beam elements.

The material properties for masonry and steel structures are those defined in the previous sections. In the FE model, the horizontal loads T_1 and T_2 , having the same value of 22.5 KN, replace the equivalent seismic load as previously

Fig. 23 Aerial view of the south wall and the adjacent courtyard

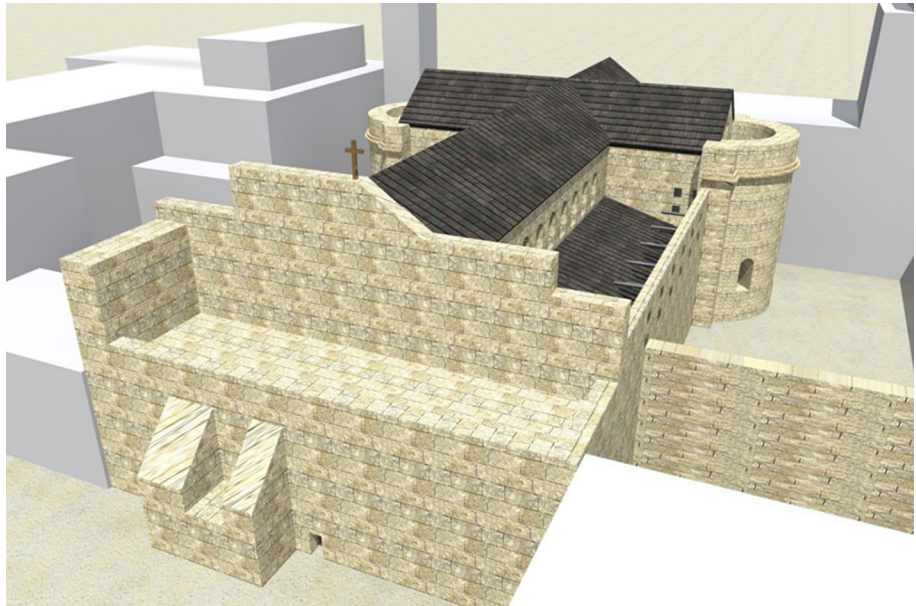


Fig. 24 The south wall from the visitors' point of view



explained in Sect. 7. The simple overturning collapse mechanism was found to be that most likely to occur, and the wall was constrained at the base in such a way as to rotate either around the external edge, when the seismic loads are directed outwards (Fig. 25), or around the internal edge, when they are directed inwards toward the Church (Fig. 26). All nodes in the two vertical sides had their longitudinal displacements impeded to take into account the presence of the orthogonal walls.

In both cases, a linear analysis was carried out for incremental values of the tension in the cables up to the value

corresponding to a maximum horizontal displacement lower than the one provided by [20] in a non-linear kinematic analysis (11.1 cm).

Table 10 refers to inward-oriented seismic actions, and shows the percentage reduction of the maximum horizontal displacement corresponding to successive increments of the tension in the cables, starting from the maximum displacement (264.30 mm) corresponding to the design earthquake with no tension in the cables. The maximum tension corresponding to a horizontal displacement lower than that

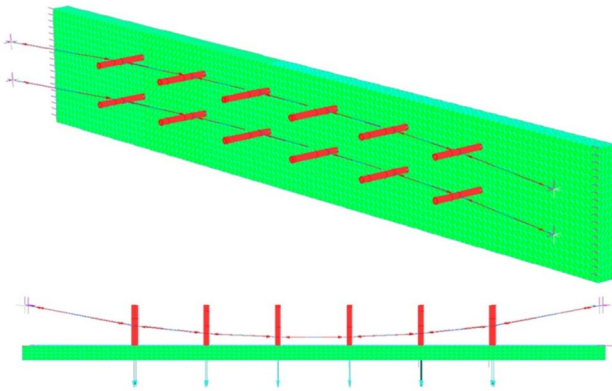


Fig. 25 FE model with outward-oriented seismic loads

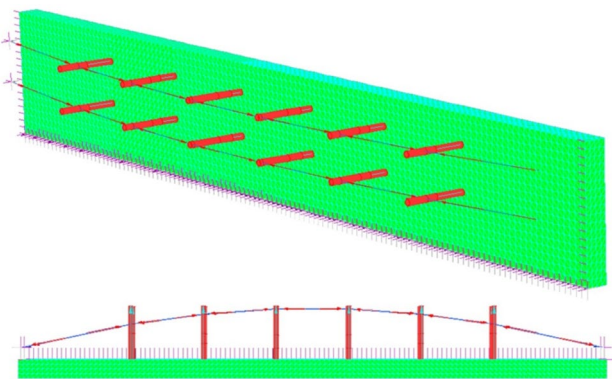


Fig. 26 FE model with inward-oriented seismic loads

admissible (11.1 cm) is 70 kN. This corresponds to a 61% reduction of the initial maximum displacement.

Table 11, on the other hand, refers to outward-oriented seismic actions at an initial maximum displacement equal to 121.50 mm, corresponding to the design earthquake with no tension in the cables. An abundantly lower displacement than that admissible is obtained in correspondence with a 50-kN tension in the cables.

The tension in the cables differs between the two cases. This is due to the weight of the steel structure, acting on the internal side, which behaves as a stabilizing load for outward-oriented actions (corresponding to a lower tension) and as an overturning load for inward-oriented actions (corresponding to a higher tension). However, the effect of such a difference in tension on the wall is irrelevant, as proved by the analysis carried out only in the presence of such tensions and the wall's own weight. In fact, it provides a maximum outward horizontal displacement of just under 2 mm.

The wall was then analysed under each type of seismic load, own weight and tensions in the cables, as computed previously, all acting simultaneously. For inward-oriented seismic loads, the maximum horizontal displacement is

Table 10 Horizontal Y displacements corresponding to inward-oriented seismic actions

Tension (kN)	Displacement in Y direction (mm)	Displacement reduction (%)
0	264.30	–
10	241.00	8.82
50	147.90	44.04
60	124.60	52.86
70	101.30	61.67

Table 11 Horizontal displacements corresponding to outward-oriented seismic actions

Tension (kN)	Displacement in Y direction (mm)	Displacement reduction (%)
0	121.50	–
10	101.40	16.54
50	20.80	82.88
60	–8.40	–
70	–29.50	–

4.52 cm, whereas for outward-oriented seismic loads it is 3.73 cm. Both values are considerably lower than the admissible value of 11.1 cm.

In the absence of reliable Palestinian technical regulations, every component of the steel structure was checked and verified according to the Italian standards [19]. All checks yielded satisfactory results.

9 Conclusions

An innovative technique was proposed for the structural consolidation of the additional masonry wall erected on top of the south wall of the Church of the Nativity in Bethlehem at the time of the Crusades. The need for such consolidation stems from the high seismic vulnerability of the wall, which endangers the safety of visitors and also the recently restored roof of the south aisle.

3D modal analysis of the entire Church using Straus7 FE code and the geometric and materials data from previous onsite surveys campaigns and investigations, as well as purpose-defined parameters corresponding to the local seismicity, clearly show that the Church is characterized by some significant local modes of vibration, like the ones of the wall examined, which justify the use of local analyses.

For this reason, and due to the peculiar behaviour of masonry structures in general and the geometric characteristics of the Church as a whole, limit analysis based on the equilibrium of macro-elements corresponding to local

collapse mechanisms was deemed more suitable than more sophisticated pushover and non-linear analyses. Owing to the weak connections of the wall with both the underlying wall of the south aisle and the two orthogonal walls of the transept and façade, a simple overturning around one edge of the base was chosen as the collapse mechanism with the highest probability of occurring.

An innovative consolidation technique was designed to prevent this happening, in full conformity to the main principles of restoration, such as lightness, non-invasiveness and reversibility. This featured two tension-structure systems acting on the horizontal plane, each of which made of pre-tensed cables with opposing curvatures, applied to the inner surface of the wall by means of horizontal steel tubes as supports for the cables. In the design, the tubes and cables are anchored to the walls by means of square steel plates and threaded steel bars embedded in the masonry.

The loads transferred by the tubes to the wall were computed on a portion of the wall constrained along one edge of the base and in equilibrium under the above-mentioned loads, the wall's own weight, and the equivalent seismic load. The same FE code and a linear elastic analysis were used to calculate the pre-tension in the cables that would allow the maximum horizontal displacement on the top of the wall, lower than that admissible, in the presence of wall and tension-structure own weights and equivalent seismic loads, increased for safety reasons. The same wall was then analysed under all applied loads, i.e. the seismic loads, inward- and outward-oriented, own weight and cable pre-tensions, all acting simultaneously. Every construction detail was checked and verified on the basis of standard procedures.

Because of the lack of appropriate and reliable local regulations, all analyses, computations and checks were carried out with reference to the Italian regulations, and all results were satisfactory. Furthermore, the proposed tension-structure system can be built without damaging the restored roof of the south aisle, as it requires no bulky or heavy scaffolding and its maintenance can easily be guaranteed through periodic checks. Indeed, after consolidation, it would be advisable to start monitoring the vulnerability of the wall and its dynamic characteristics by new, recently developed techniques, like those based on micro-tremor measurements [31].

Acknowledgements Thanks are due to Piacenti S.p.A., the main contractor for the restoration works on the Church of the Nativity, and to all their staff, for providing geometric and materials data. The first Author is also grateful to the Palestinian Presidential Committee for the restoration works on the Church of the Nativity for his appointment as general consultant for the ongoing restoration works, and the opportunity to contribute to the studies on the Church.

References

- Alessandri C (2012) Preface. *J Cult Herit* 13:e1–e4
- Bacci M, Bianchi G, Campana S, Fichera G (2012) Historical and archaeological analysis of the Church of the Nativity. *J Cult Herit* 13:e5–e26
- Santopuoli N, Concina E, Sarmati S (2012) The conservation of the Church of the Nativity in Bethlehem and the preliminary restoration project of the decorated surfaces. *J Cult Herit* 13:e93–e123
- Faella G, Frunzio G, Guadagnuolo M, Donadio A, Ferri L (2012) The Church of the Nativity in Bethlehem: non-destructive tests for the structural knowledge. *J Cult Herit* 13:e27–e41
- Macchioni N, Brunetti M, Pizzo B, Burato P, Nocetti M, Palanti S (2012) The timber structures in the Church of the Nativity: typologies and diagnosis. *J Cult Herit* 13:e42–e53
- Bernabei M, Bontadi J (2012) Dendrochronological analysis of the timber structure of the Church of the Nativity in Bethlehem. *J Cult Herit* 13:e54–e60
- Palanti S, Pecoraro E, Scarpino F (2012) Wooden doors and windows in the Church of the Nativity: evaluation of biotic and abiotic decay and proposals of interventions. *J Cult Herit* 13:e82–e92
- Alessandri C, Mallardo V (2012) Structural assessments of the Church of the Nativity in Bethlehem. *J Cult Herit* 13:e61–e69
- Alessandri C, Mallardo V, Pizzo B, Ruocco E (2012) The roof of the Church of the Nativity in Bethlehem: structural problems and intervention techniques. *J Cult Herit* 13:e70–e81
- Mele E, De Luca A, Giordano A (2012) Modelling and analysis of a basilica under earthquake loading. *J Cult Herit* 4:355–367
- Papalou A (2016) Examining the dynamic response of classical columns. *Int J Civ Eng*. doi:10.1007/s40999-016-0110-6
- Lagomarsino S, Podestà S (2004) Seismic vulnerability of ancient churches: I. Damage assessment and emergency planning. *Earthq Spectra* 20(2):377–394
- Mallardo V, Malvezzi R, Milani E, Milani G (2008) Seismic vulnerability of historical masonry buildings: a case study in Ferrara. *Eng Struct* (30):2223–2241
- Milani G, Del Grosso A, Alessandri C, Valente M (2015) A non-linear finite element approach to predict the structural damage of the Narthex of the Bethlehem Nativity Church. In: *Proceedings of the fifteenth international conference on Civil-Comp Press*, pp 1–16
- Choi HK, Bae BI, Choi CS (2016) Lateral resistance of unreinforced masonry walls strengthened with engineered cementitious composite. *Int J Civ Eng* 14:411. doi:10.1007/s40999-016-0026-1
- Hamilton RW (1934) Excavations in the Atrium of the Church of the Nativity. *Q Dep Antiq Palest* (3):1–8
- Harvey W (1938) Recent discoveries at the Church of the Nativity, Bethlehem. *Archaeologia* (87):7–17
- Bagatti B (1952) Gli antichi edifici sacri di Betlemme, Jerusalem
- Decreto Ministeriale 14 Gennaio 2008 “Norme Tecniche per le Costruzioni” e relativi allegati A e B, pubblicato nel Supplemento ordinario della Gazzetta Ufficiale n. 29 del 4 Febbraio 2008
- Consiglio Superiore dei Lavori Pubblici—Circolare 2 febbraio 2009, n. 617—Istruzioni per l'applicazione delle “Nuove Norme Tecniche per le Costruzioni” di cui al D.M. 14 gennaio 2008
- Consiglio Superiore dei Lavori Pubblici—Linee Guida per la valutazione e riduzione del rischio sismico del patrimonio culturale—allineamento alle nuove Norme tecniche per le costruzioni (23 luglio 2010)
- (2004) Straus7—finite element analysis system release 2.3.3

23. Brandonisio G, Lucibello G, Mele E, De Luca A (2013) Damage and performance evaluation of masonry churches in the 2009 L'Aquila earthquake. *Eng Fail Anal* 34:693–714
24. Milani G, Valente M (2015) Comparative pushover and limit analyses on seven masonry churches damaged by the 2012 Emilia-Romagna (Italy) seismic events: possibilities of non-linear finite elements compared with pre-assigned failure mechanisms. *Eng Fail Anal* 47:129–161
25. Milani G, Valente M (2015) Failure analysis of seven masonry churches severely damaged during the 2012 Emilia-Romagna (Italy) earthquake: non-linear dynamic analyses vs conventional static approaches. *Eng Fail Anal* 54:13–56
26. Valente M, Milani G (2016) Seismic assessment of historical masonry towers by means of simplified approaches and standard FEM. *Constr Build Mater* 108:74–104
27. Milano L, Mannella A, Morisi C, Martinelli A (2009) Schede illustrative dei principali meccanismi di collasso locali negli edifici esistenti in muratura e dei relativi modelli cinematici di analisi, ReLUIS, Allegato alle Linee Guida per la Riparazione e il Rafforzamento di Elementi Strutturali, Tamponature e Partizioni
28. Mc4 Loc Software (2014) L'analisi dei meccanismi locali (technical manual)
29. Munari M, Bettiol G, Da Porto F, Milano L, Modena C (2010) Esempio di calcolo su rafforzamento locale di edifici in muratura con tiranti, ReLUIS, Allegato alle Linee Guida per la Riparazione e il Rafforzamento di Elementi Strutturali, Tamponature e Partizioni (updated version)
30. Jurina L (2012) Il consolidamento del Duomo di Cremona, Politecnico di Milano, DIS
31. Hadianfard MA, Rabiee R, Sarshad A (2016) Assessment of vulnerability and dynamic characteristics of a historical building using microtremor measurements. *Int J Civ Eng*. doi:[10.1007/s40999-016-0086-2](https://doi.org/10.1007/s40999-016-0086-2)